

Mode locking of a wavelength-swept laser

Seok Hyun Yun

Harvard Medical School and Wellman Center for Photomedicine, Massachusetts General Hospital, 50 Blossom Street, BAR 718, Boston, Massachusetts 02114

Received May 6, 2005; accepted June 17, 2005

Self-starting, stable mode-locked pulses can be generated from a wavelength-swept laser through the interplay between an intracavity scanning filter and self-phase modulation. From an Er^{3+} -doped fiber laser employing a scanning Fabry–Perot filter, 100 ps optical pulses are obtained at a 12-MHz repetition rate with center wavelengths that are swept over 27 nm around 1.55 μm in 1 ms. © 2005 Optical Society of America
OCIS codes: 140.4050, 140.3510, 140.3600.

Tunable lasers typically employ intracavity spectral filters. Sweeping the center frequency of the filter rapidly and repeatedly across the broad spectral range supported by the laser gain medium can result in a wavelength-swept output spectrum. These wavelength-swept lasers are of practical interest for various applications, including sensing,^{1,2} spectroscopy, reflectometry,^{3,4} and biomedical imaging.⁵

Single-longitudinal-mode wavelength swept operation can be achieved if the swept filter is used in conjunction with a modulation of laser cavity length or an intracavity frequency shifter that precisely tracks the center frequency of the swept filter. Such lasers have been successfully realized using temperature tuning⁶ or grating filters in the Littman configuration,⁷ resulting in relatively low sweep repetition rates below 10 Hz. Rapidly swept lasers employing scanning filters, however, intrinsically produce output spectra consisting of multiple longitudinal modes.^{1,3,8} In a simple frequency–time-domain picture,^{9,10} the oscillating spectrum follows the moving passband of the filter through the creation of new modes at the leading filter edge and annihilation of old modes at the trailing filter edge.

If each of the modes originated from incoherent spontaneous emission, they would be randomly phased and would produce continuous-wave (cw) radiation. However, a defined phase relationship among the modes can be achieved if the intracavity light undergoes sufficient self-phase modulation providing coherent seed photons for the new modes. This mode-locking mechanism was originally demonstrated in frequency-shifted-feedback fiber lasers employing intracavity frequency shifters and fixed spectral filters.^{10,11} In this Letter, the mode-locking mechanism is demonstrated in a wavelength-swept fiber laser that uses the interplay between a scanning filter and self-phase modulation,⁹ termed sliding-frequency mode locking. The result is a mode-locked laser producing a series of 100 ps optical pulses in which the center wavelength of each pulse is incremented or decremented by a controllable amount. The overall wavelength range of the pulse series is 27 nm around 1550 nm, and the wavelength sweep rate can be as high as 1 kHz.

Figure 1 shows a schematic of the λ -swept fiber laser.² The unidirectional ring cavity comprises single-mode fibers (SMF28), isolators, a tunable

bandpass filter, and an Er^{3+} -doped fiber (EDF). The EDF is 6.3 m in length and has a small signal absorption coefficient of 12 dB/m at 1530 nm. The pump diode at 1470 nm delivers up to 70 mW in the EDF through the wavelength-division multiplexer. The intracavity filter is a fiber-based, air-gap Fabry–Perot tunable filter with a 3 dB bandwidth of 0.23 nm and a free-spectral range of 33 nm. The center wavelength of the filter is swept from 1538 to 1565 nm by a triangle-waveform driving signal at frequencies from DC to 1 kHz. The maximum tuning speed is limited by the finite response time of the filter. The total cavity length is 16.8 m, corresponding to a longitudinal mode spacing of 12.2 MHz. The total cavity loss, excluding the EDF gain, is estimated to be 10 dB, including 4 dB in the filter, 3 dB in the output coupler, and 2 dB at splices and connectors. The mode size in the EDF is 10 μm^2 , smaller than the 50 μm^2 mode size in the single-mode fiber. Therefore, it is expected that self-phase modulation takes place mostly within the last few meters of the EDF, where the optical intensity is highest.

When the filter was not scanned, the laser produced cw radiation if the launched pump power levels exceeded a lasing threshold of 4 mW. Figure 2(a) shows the output power (dotted line) measured with the filter fixed at 1550 nm. In the swept operation, the laser exhibited various output regimes as a function of the pump power (Fig. 2). At pump powers below a mode-locking threshold of 25 mW, the laser produced cw radiation with large intensity fluctua-

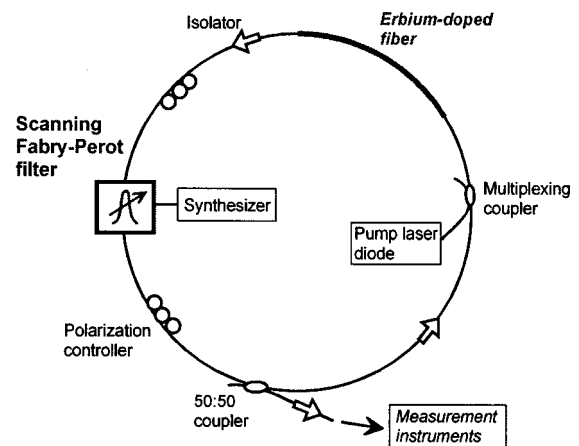


Fig. 1. Schematic of the wavelength-swept fiber laser.

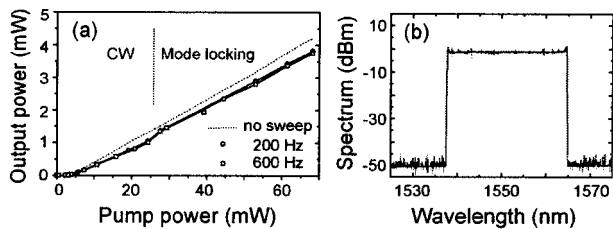


Fig. 2. (a) Average output power and (b) peak-hold spectrum.

tions resulting mainly from relaxation oscillations at several tens of kHz. These fluctuations increased as the pump power increased until the laser output became chaotic at pump powers just below the mode-locking threshold. At pump powers above this threshold, mode locking started spontaneously. The kink in the slope efficiency evident in Fig. 2 indicates that the effective filtering loss is smaller in the mode-locked state than in the cw state. Weak but noticeable hysteresis in the slope efficiency was observed at the mode-locking threshold. The mode-locked state was stable over a time period of the order of several hours at sweep rates of 150–1000 Hz and pump powers of 30–50 mW. At lower sweep rates of several to 100 Hz, mode-locked operation was frequently interrupted by a cw output state with a time scale of <1 s. At pump powers higher than 60 mW, mode-locked operation became unstable, sometimes yielding two or three pulses per round trip.¹⁰

Figure 3 shows an oscilloscope trace of the laser output pulses at a pump power of 36 mW and a sweep frequency of 250 Hz. The laser center wavelength increases as the voltage applied to the filter (triangular waveform) increases. The pulse repetition rate is 12.2 MHz. The separation of two neighboring pulses is 83 ns in time, 1.1 pm in wavelength, and 140 MHz in optical frequency. All the optical components in the cavity were nominally polarization independent. At some settings of the intracavity polarization controllers, the output polarization state exhibited rapid variations in time, or wavelength, within each sweep. This phenomenon arises due to cavity birefringence and can be explained by simultaneous oscillations of two uncorrelated polarization eigenmodes. Mode-locked operation started spontaneously at all settings of the polarization controllers. In a separate experiment, the wavelength-dependent polarization evolution could be suppressed through the insertion of an intracavity fiber polarizer (20 cm, 2 dB extinction).

The peak power traces are nearly identical when one compares wavelength sweeps in the same direction but differ between increasing (down-sliding-frequency) and decreasing (up-sliding-frequency) sweeps. This difference results from a variation in the chromatic dispersion across the Fabry–Perot filter passband.¹² To understand this, we numerically simulated our laser using a model described previously.^{9,10} Briefly, the model uses a split-step Fourier method and includes optical amplification, spontaneous emission, spectral filtering, the nonlinear Kerr effect, and chromatic dispersion. The computer simulation predicted self-starting mode-locked

pulses in the presence of both a λ -swept filter and self-phase modulation, and cw radiation otherwise. The nonlinear phase shift accumulated at the peak of the pulse was found to be 0.14 rad per round trip at a pump power of 36 mW. The chromatic dispersion of the optical fiber in the cavity was nearly two orders of magnitude smaller than that induced by the Fabry–Perot filter and therefore played a negligible role. The chromatic dispersion of the filter is negative (anomalous) at frequencies above its center frequency and positive at frequencies below its center frequency. This asymmetry produced the difference in the intensities and temporal and spectral characteristics of pulses originating during up- and down-sliding operations. Because the center of the lasing spectrum tends to be displaced from, lagging behind, the center of the filter passband in the swept operation,⁹ down-sliding operation causes the lasing spectrum to overlap more with the anomalous dispersion region and therefore produces narrower pulses than up-sliding operation. When the chromatic dispersion was neglected by using only the real part of the filter function, the two scan directions produced identical results.

In the experiment, the average pulse width between up- and down-sliding operations was measured with a second-harmonic generation autocorrelator. The spectral width of the pulses was calculated from a Gaussian fit to the coherence function measured with a variable-delay Michelson interferometer. The experimental results, measured at several sweep rates, correspond reasonably well with the simulation, as depicted in Fig. 4. The simulation produced shorter pulses than the experimental results but correctly predicted the dependence on the tuning speed and the difference between up- and down-sliding operations. The measured time-bandwidth product was 0.46, averaged between up- and down-sliding. The predicted value by simulation was 0.48 for up-sliding and 0.43 for down-sliding.

The common nature of sliding-frequency mode locking in both wavelength-swept and frequency-shifted-feedback operations is further elucidated in the following experiment. A fiber-pigtailed, acousto-optic frequency shifter was inserted into the laser cavity and provided an intracavity optical frequency shift of 108 MHz. During up-sliding operation at a sweep rate of 77 Hz, the filter sliding speed is matched to the intracavity frequency shift. As a result, the effective sliding speed seen by the intracavity light is zero and a frustration of the mode-locked operation is anticipated. This behavior was measured

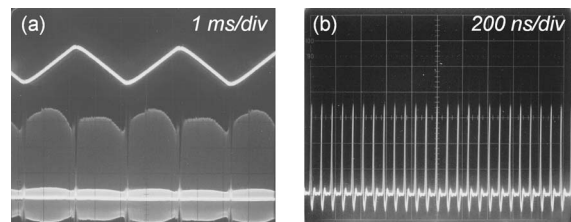


Fig. 3. (a) Oscilloscope trace of the laser output and the driving signal applied to the filter (upper trace). (b) Mode-locked pulses.

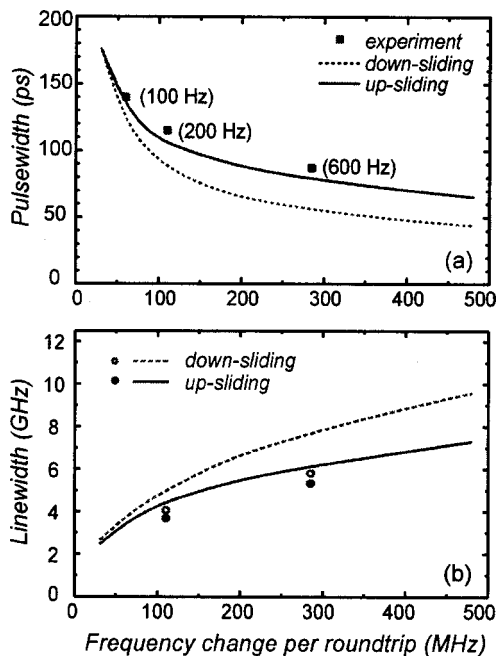


Fig. 4. (a) Temporal and (b) spectral widths of the pulses. Data points, experimental results; lines, numerical simulations.

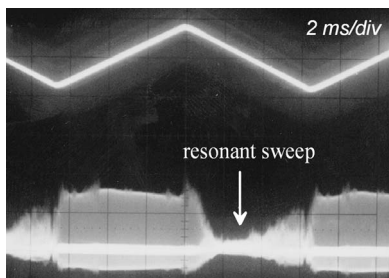


Fig. 5. Laser output in the presence of an intracavity frequency shifter. A frustration of mode locking is observed when the tuning speed and direction are matched to the frequency shift (resonant sweep), resulting in cw emission.

and is shown in Fig. 5. During down-sliding operation at the same tuning speed, the effective sliding speed is 216 MHz (twice the frequency shift) per round trip, and the laser again generates stable mode-locked pulses.

It has been shown that wavelength-swept pulses can be generated by sliding frequency mode locking without the need for conventional mode lockers such as amplitude modulators or saturable absorbers. In addition, our simulations show that the generation of picosecond or subpicosecond pulses might be possible through optimization of the spectral width and scan speed of a filter and the level of intracavity nonlinearity. Rapidly swept mode-locked lasers such as these are expected to find applications in biomedical imaging based on multiphoton interactions in biological samples or time-resolved spectroscopy.

The author thanks B. Y. Kim of the Korea Advanced Institute of Science and Technology for his support. The experiments were conducted in his laboratory. S. H. "Andy" Yun's e-mail address is syun@hms.harvard.edu.

References

1. P. F. Wysocki, M. J. Dignonnet, and B. Y. Kim, *Opt. Lett.* **15**, 879 (1990).
2. S. H. Yun, D. J. Richardson, and B. Y. Kim, *Opt. Lett.* **23**, 843 (1998).
3. B. Golubovic, B. E. Bouma, G. J. Tearney, and J. G. Fujimoto, *Opt. Lett.* **22**, 1704 (1997).
4. B. J. Soller, D. K. Gifford, M. S. Wolfe, and M. E. Froggatt, *Opt. Express* **13**, 666 (2005).
5. S. H. Yun, G. J. Tearney, J. F. de Boer, N. Iftimia, and B. E. Bouma, *Opt. Express* **11**, 2953 (2003).
6. W. V. Sorin, D. K. Donald, S. A. Newton, M. Nazarthy, *IEEE Photon. Technol. Lett.* **2**, 902 (1990).
7. K. Liu and G. Littman, *Opt. Lett.* **6**, 117 (1981).
8. S. H. Yun, C. Boudoux, G. J. Tearney, and B. E. Bouma, *Opt. Lett.* **28**, 1981 (2003).
9. S. H. Yun, D. J. Richardson, D. O. Culverhouse, and B. Y. Kim, *IEEE J. Sel. Top. Quantum Electron.* **3**, 1087 (1997).
10. H. Sabert and E. Brinkmeyer, *J. Lightwave Technol.* **12**, 1360 (1994).
11. F. Fontana, L. Bossalini, P. Franco, M. Midrio, M. Romagnoli, and S. Wabnitz, *Electron. Lett.* **30**, 321 (1994).
12. E. A. Golovchenko, A. N. Pilipetskii, C. R. Menyuk, J. P. Gordon, and L. F. Mollenauer, *Opt. Lett.* **20**, 539 (1995).